Multiband terahertz metamaterial absorber*

Gu Chao(顾 超)[a], Qu Shao-Bo(屈绍波)[a)b)†], Pei Zhi-Bin(裴志斌)[a], Xu Zhuo(徐 卓)[b], Liu Jia(刘 嘉)[a], and Gu Wei(顾 巍)[c]

[a] *The College of Science, Air Force University of Engineering, Xi'an* 710051, *China*
[b] *Electronic Materials Research Laboratory, Key Laboratory of Ministry of Education, Xi'an Jiaotong University, Xi'an* 710049, *China*
[c] *The Engineering and Technical College of Chengdu University of Technology Department of Computer Science and Technology, Leshan* 614300, *China*

(Received 30 March 2010; revised manuscript received 19 May 2010)

This paper reports the design of a multiband metamaterial (MM) absorber in the terahertz region. Theoretical and simulated results show that the absorber has four distinct and strong absorption points at 1.69, 2.76, 3.41 and 5.06 THz, which are consistent with 'fingerprints' of some explosive materials. The retrieved material parameters show that the impedance of MM could be tuned to match approximately the impedance of the free space to minimise the reflectance at absorption frequencies and large power loss exists at absorption frequencies. The distribution of the power loss indicates that the absorber is an excellent electromagnetic wave collector: the wave is first trapped and reinforced in certain specific locations and then consumed. This multiband absorber has applications in the detection of explosives and materials characterisation.

Keywords: multiband, terahertz, electromagnetic resonance, metamaterial absorber
PACS: 78.20.Ci, 41.20.Jb **DOI:** 10.1088/1674-1056/20/1/017801

1. Introduction

Metamaterial (MM) has produced exotic effects such as negative index of refraction,[1,2] and devices such as an electromagnetic (EM) cloak.[3] The realisation of such properties lies in the ability of MM to create independent tailored electric[4] and magnetic[5] responses to incident radiation. The MM is also geometrically scalable, which translates into operability over a significant portion of the EM spectrum. So far, MM has been demonstrated in every technologically relevant spectral range, from radio,[6] microwave,[7,8] mm-Wave,[9] THz,[10] middle infrared ray (MIR),[11] near infrared ray (NIR),[12] to the near optical.[13] It is ideal for the investigation of novelly emergent physical phenomena while also holding great promise for future applications.

Recently, the design of resonant metamaterial absorber (MA) at microwave and terahertz (THz) bands has attracted much attention. By adjusting the dimensions of MM, a 'perfect' MA with near-unity absorption can be realised in the GHz regime.[14,15] In the THz regime, several MAs have been presented.[16−18] However, almost all existing THz MAs have single-band or double-band response, which limits their potential applications in detection of explosives and materials characterisation.[19−21] Explosive marerials absorb the light strongly at certain THz frequencies but not at others, and this 'THz fingerprint' can be used to identify an explosive, and distinguish it from clothing or other inert materials. So a THz absorber with strong multifrequency absorption is desirable, but still lacking so far. In this work, we propose an MA that has strong multifrequency absorption in the THz region. The special feature of this MA is that its absorption frequencies are consistent with 'fingerprints' of some explosive materials. Both theoretical and simulated results reveal that MA has four distinct and strong absorption points near 1.69, 2.76, 3.41 and 5.06 THz, all of which are related to the EM resonance of MM.

2. Design and simulation

A single unit cell of the MA consisted of two distinct metallic elements as shown in Figs. 1(a) and 1(b). Electric coupling was supplied by the electric split-ring resonator (ESRR), shown in Fig. 1(a). Magnetic

*Project supported by the National Natural Science Foundation of China (Grant Nos. 60871027, 60901029 and 61071058), the National Basic Research Program of China (Grant No. 2009CB623306) and Key Laboratory of Shaanxi Provincial Synthetic Electronic Information System Foundation, China (Grant No. 200905A).
†Corresponding author. E-mail: 15929560875@139.com
© 2011 Chinese Physical Society and IOP Publishing Ltd

coupling was supplied by the coupling of inner continuous wires of the ESRR [Fig. 1(a)] and cut wires [Fig. 1(b)] between two parallel planes separated by a substrate as shown in Fig. 1(c). This design is similar to short wire pairs,[22] in that they derive a magnetic response from driving two antiparallel currents in conducting segments. We were then able to tune the EM response by changing the dimensions of ESRR, cut wires and the separation between them. To maximise the absorption of the device, the reflection should be minimised. So the impedance of the MA should be tuned to match approximately the impedance of the free space to minimise the reflectance at absorption frequencies.

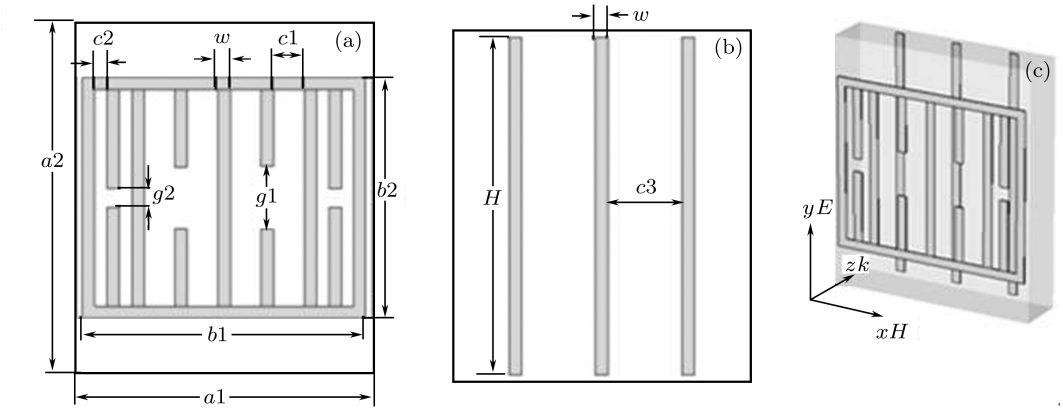


Fig. 1. The ESRR (a) and cut wires (b). Dimension notations are listed in (a) and (b). The unit cell is shown in (c) with axes indicating the propagation direction.

We performed computer simulations of the MA using the commercial finite difference time domain solver (CST Microwave Studio). The programme simulated a single unit cell as shown in Fig. 1(c) with proper boundary conditions, i.e., perfect electric boundary (xz-plane) and perfect magnetic boundary (yz-plane). Waveguide ports on the other boundaries simulated a TEM plane wave propagating through the medium. Using CST, the structure of the MA was optimised (simulating radiation at a normal incidence with the electric field parallel to cut wires) and the obtained size parameters were listed in the caption of Figs. 1(a) and 1(b), which had the dimensions, in micron, of $c1 = 4.5$, $c2 = 1$, $g1 = 1.2$, $g2 = 0.8$, $a1 = 83$, $a2 = 36$, $b1 = 81$, $b2 = 26.5$, $w = 6.5$, $c3 = 15.5$ and $H = 35.5$. The substrate is 8 μm thick, ($\varepsilon = 4.9$, $t\mathrm{d} = 0.025$). Simulation produced the complex frequency dependent S parameters, S_{11} and S_{21}, where $R(\omega) = |S_{11}|^2$, $T(\omega) = |S_{21}|^2$ and $A(\omega) = 1 - |S_{11}|^2 - |S_{21}|^2$ are the reflectance, transmission and absorbance respectively, as shown in Fig. 2.

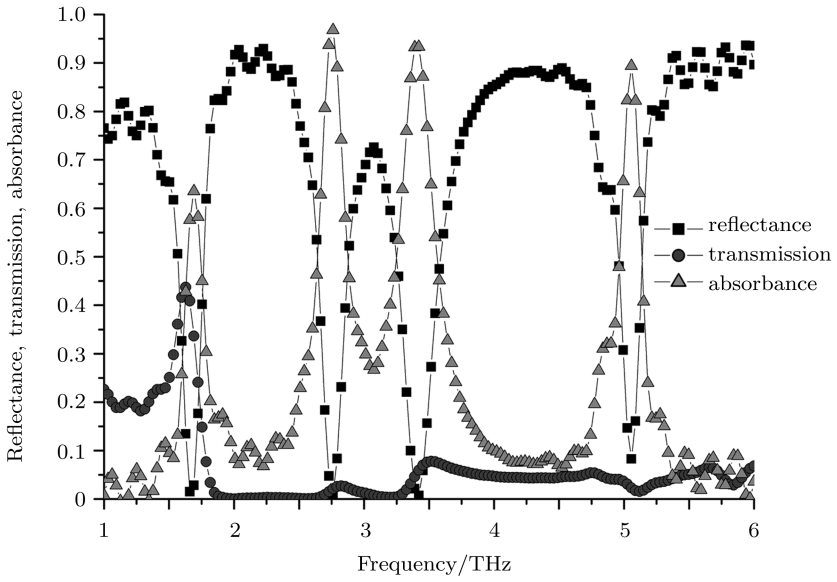


Fig. 2. Simulated MA's $R(\omega)$, $T(\omega)$ and $A(\omega)$ are plotted from zero to 100%.

From Fig. 2, we could see that there are four distinct absorptive peaks located at 1.69, 2.76, 3.41 and 5.06 THz, with absorption 63.5%, 97.1%, 94.1% and 89.4% respectively. The absorption bandwidths, defined as full width at half maximum, are 0.1, 0.23, 0.31 and 0.17 THz for the four absorptive peaks. These results indicate the strong frequency selectivity of our MA.

Then we could retrieve the values for the complex wave impedance Z, refractive index n, effective permeability μ and effective permittivity ε from the simulated S parameters, as shown in Fig. 3. From Fig. 3(a), we can see that the real parts of our retrieved impedance at four absorptive peaks are 1.16, 1.20, 0.89 and 0.57, which are consistent with our intent to match approximately the impedance to the free space to minimise the reflectance at absorptive frequencies. From Figs. 3(c) and 3(d), we could see that the real parts of our retrieved permeability and permittivity at four absorptive peaks are at close range, which is consistent with the retrieved impedance in Fig. 3(a). From Fig. 3(b), peaks of imaginary part of refractive index present at absorption frequencies, which indicate large power loss.

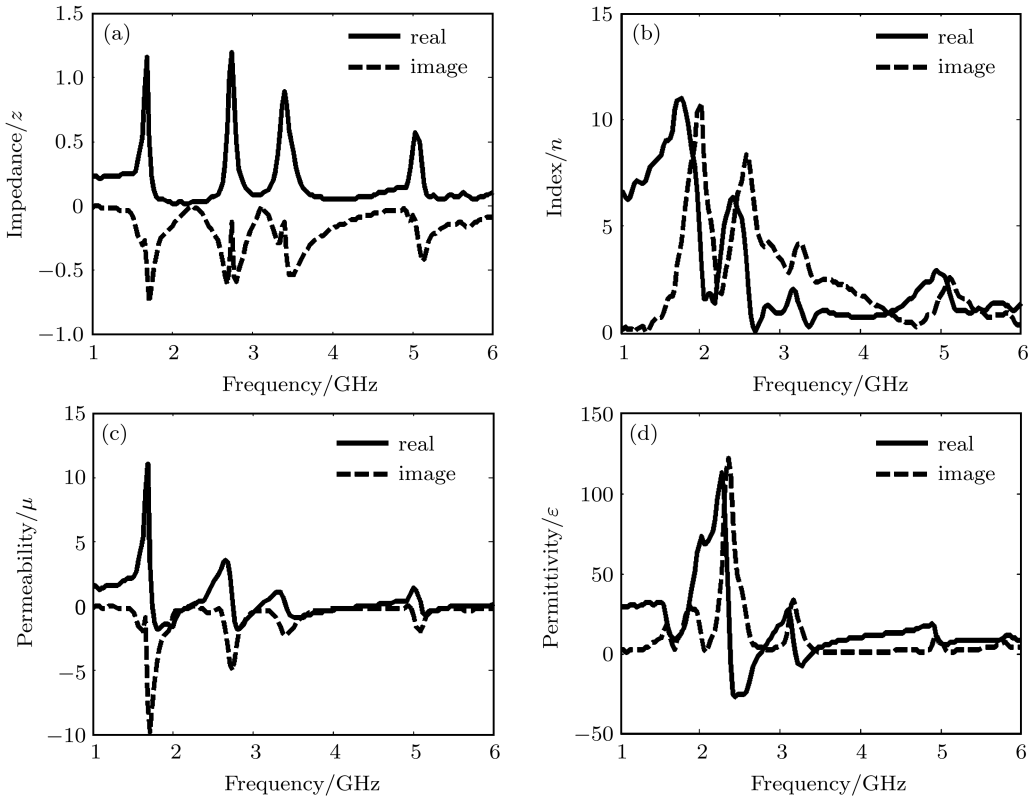


Fig. 3. (a) Retrieved impedance, (b) retrieved refractive index, (c) retrieved permeability, (d) retrieved permittivity.

3. The distribution of the power loss

It is also interesting to explore the power loss since it can provide information about how and where the absorption happens. The distribution of the power loss in the MA was calculated and compared for the four absorption frequencies, as shown in Fig. 4. Figures 4(a), 4(c), 4(e) and 4(g) are the front views of the power loss on the xy-plane. The top views of the power loss on the x-z plane, as plotted in Figs. 4(b), 4(d), 4(f) and 4(h), provide detailed information of the absorption that occurred in different layers. For the 1.69 THz absorption [Figs. 4(a) and 4(b)], the power loss mainly takes place in cuts of cut wires and the neighbouring substrate. For the 2.76 THz absorption [Figs. 4(c) and 4(d)], the power loss mainly takes place in splits at the centre of ESRR and the neighbouring substrate. For the 3.41 THz absorption [Figs. 4(e) and 4(f)], most of the power loss occurs at splits at the two sides of ESRR and the neighbouring substrate. For the 5.06 THz absorption [Figs. 4(g) and 4(h)],

most of the power loss occurs at the cuts of the middle cut wires and the neighbouring substrate. In conclusion, we can deduce that the MA can concentrate the EM wave in some specified locations, where the energy is significantly reinforced and subsequently converted into thermal energy, leading to strong absorption.

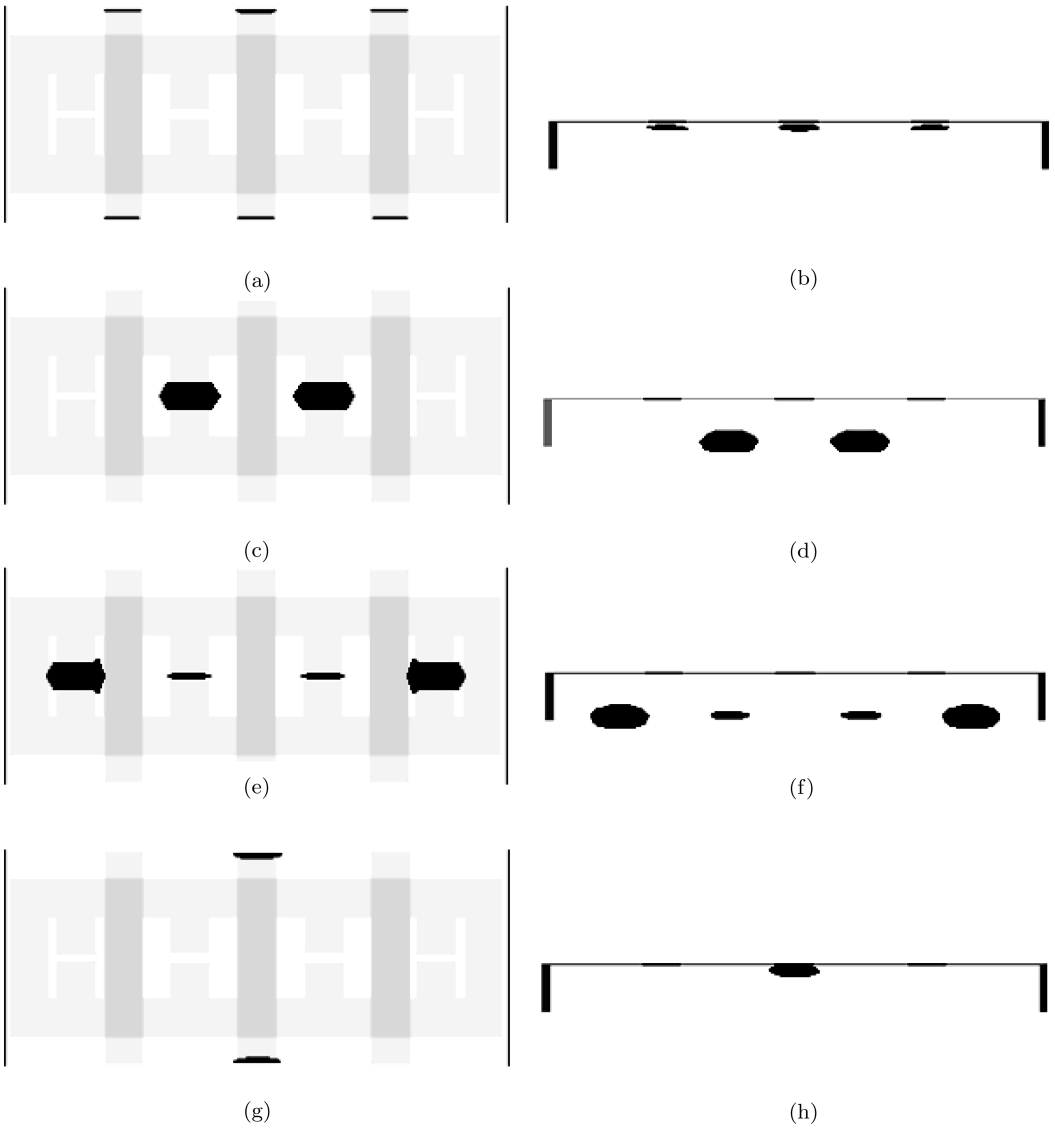


Fig. 4. The distribution of the power loss in the MA. The front view for (a) 1.69, (c) 2.76, (e) 3.41 and (g) 5.06 THz, and the top view for (b) 1.69, (d) 2.76, (f) 3.41 and (h) 5.06 THz.

4. Conclusion

In summary, we present an MA that has four distinct absorptions of 63.5%, 97.1%, 94.1% and 89.4% near 1.69, 2.76, 3.41 and 5.06 THz respectively. The special feature of this MA is that its absorption frequencies are consistent with 'fingerprints' of explosive materials. The retrieved impedance shows that the impedance of MM could be tuned to match approximately the impedance of the free space to minimise the reflectance at absorption frequencies. The retrieved refractive index indicates the existence of large power loss at absorption frequencies. The absorption mechanism was theoretically investigated by simulating power loss, which indicates that the absorber is an excellent electromagnetic wave collector, which traps the input EM wave into specific locations and then strongly absorbs it.

The design presented here can still be improved. The current design is polarisation sensitive, which is not ideal for some applications. By improving the symmetry of MM cell, the polarisation sensitivity can be depressed.

References

[1] Veselago V G 1968 *Sov. Phys. Usp.* **10** 509

[2] Shelby R A, Smith D R and Schultz S 2001 *Science* **292** 77

[3] Schurig D, Mock J J, Justice B J, Cummer S A, Pendry J B, Starr A F and Smith D R 2006 *Science* **314** 977

[4] Pendry J B, Holden A J, Stewart W J and Youngs I 1996 *Phys. Rev. Lett.* **76** 4773

[5] Pendry J B, Holden A J, Robbins D J and Stewart W J 1999 *IEEE Trans. Microwave Theory Tech.* **47** 2075

[6] Wiltshire M C K, Pendry J B, Young I R, Larkman D J, Gilderdale D J and Hajnal J V 2001 *Science* **291** 849

[7] Smith D R, Padilla W J, Vier D C, Nemat-Nasser S C and Schultz S 2000 *Phys. Rev. Lett.* **84** 4184

[8] Zhang S, Qu S B, Ma H, Xie F and Xu Z 2009 *Acta Phys. Sin.* **58** 3961 (in Chinese)

[9] Gokkavas M, Guven K, Bulu I, Aydin K, Penciu R S, Kafesaki M, Soukoulis C M and Ozbay E 2006 *Phys. Rev.* B **73** 193103

[10] Yen T J, Padilla W J, Fang N, Vier D C, Smith D R, Pendry J B, Basov D N and Zhang X 2004 *Science* **303** 1494

[11] Linden S, Enkrich C, Wegener M, Zhou J F, Koschny T and Soukoulis C M 2004 *Science* **306** 1351

[12] Zhang S, Fan W, Panoiu N C, Malloy K J, Osgood R M and Brueck S R J 2005 *Phys. Rev. Lett.* **95** 137404

[13] Dolling G, Wegener M, Soukoulis C M and Linden S 2007 *Opt. Lett.* **32** 53

[14] Landy N I, Sajuyigbe S, Mock J J, Smith D R and Padilla W J 2008 *Phys. Rev. Lett.* **100** 207402

[15] Tao H, Landy N I, Bingham C M, Zhang X, Averitt R D and Padilla W J 2008 *Opt. Express* **16** 7181

[16] Tao H, Bingham C M, Strikwerda A C, Pilon D, Shrekenhamer D, Landy N I, Fan K, Zhang X, Padilla W J and Averitt R D 2008 *Phys. Rev.* B **78** 241103(R)

[17] Avitzour Y, Urzhumov Y A and Shvets G 2009 *Phys. Rev.* B **79** 045131

[18] Landy N I, Bingham C M, Tyler T, Jokerst N, Smith D R and Padilla W J 2009 *Phys. Rev.* B **79** 125104

[19] Wang G Q, Shen J L and Jia Y 2007 *J. Appl. Phys.* **102** 013106

[20] Zhou Q L, Zhang C L, Mu K J, Jin B, Zhang L L, Li W W and Feng R S 2008 *Appl. Phys. Lett.* **92** 101106

[21] Zhang L L, Zhong H, Deng C, Zhang C L and Zhao Y J 2008 *Appl. Phys. Lett.* **92** 091117

[22] Zhou J F, Zhang L, Tuttle G, Koschny T and Soukoulis C M 2006 *Phys. Rev.* B **73** 041101